Biodegradable Poly(ethylene succinate) Blends and Copolymers Containing Minor Amounts of Poly(butylene succinate)

Hsin-Ying Lu,[1] Ming Chen,[1] Chi He Chen,[1] Jin-Shan Lu,[1] Kim-Chi Hoang,[2] Min Tseng[3]

[1]*Department of Materials and Optoelectronic Science, National Sun Yat-Sen University, Kaohsiung 80424, Taiwan, Republic of China*
[2]*Department of Chemical and Material Engineering, Ta-Hwa Institute of Technology, Hsinchu 30743, Taiwan, Republic of China*
[3]*Bioresource Collection and Research Center, Food Industry Research and Development Institute, Hsinchu 300, Taiwan, Republic of China*

Received 1 April 2009; accepted 10 December 2009
DOI 10.1002/app.31932
Published online 22 February 2010 in Wiley InterScience (www.interscience.wiley.com).

ABSTRACT: Poly(ethylene succinate) (PES), poly(butylene succinate) (PBS), and PES-rich copolyesters were synthesized using an effective catalyst, titanium tetraisopropoxide. PES was blended with minor amounts of PBS for the comparison. The compositions of the copolyesters and the blends were determined from NMR spectra. Their thermal properties were studied using a differential scanning calorimeter (DSC), a temperature modulated DSC (TMDSC), and a thermogravimetric analyzer. No significant difference exists among the thermal stabilities of these polyesters and blends. For the blends, the reversible curves of TMDSC showed a distinct glass-rubber transition temperature (T_g), however, the variation of the T_g values with the blend compositions was small. Isothermal crystallization kinetics and the melting behavior after crystallization were examined using DSC. Wide-angle X-ray diffractograms (WAXD) were obtained for the isothermally crystallized specimens. The results of DSC and WAXD indicate that the blends have a higher degree of crystallinity and a higher melting temperature than those of the corresponding copolymers. © 2010 Wiley Periodicals, Inc. J Appl Polym Sci 116: 3693–3701, 2010

Key words: polyesters; crystallization; biodegradable

INTRODUCTION

Polymers universally used such as polyethylene (PE), polypropylene (PP), and polystyrene have caused increasingly serious pollution problem in the last several decades because of their high chemical stability. With the rise of concern about the global environment, much attention has recently been paid to environmental protection policy for every government. Biodegradable polymers[1] are friendly to our ecosystem and offer alternative solutions for solid waste management. Aliphatic polyesters are among the most interesting candidates for biodegradable materials because they can be degraded to CO_2 and H_2O by the action of enzymes and microorganisms. Poly(ethylene succinate) (PES) and poly(butylene succinate) (PBS) are attractive thermoplastics, fully biodegradable,[2] because they have relatively high melting temperature ($T_m > 103°C$) and very favorable mechanical properties, which are similar to those of such extensively used polymers as low density PE (LDPE), PP[3] and others. Moreover, PES and PBS have excellent processability, so they can be processed using conventional equipments.

PBS exhibits a lower biodegradation rate than PES because it has a higher crystallization rate and greater crystallinity. PES has been reported to be degraded by polyhydroxybutyrate (PHB) depolymerase,[4–7] and be hydrolyzed by lipase[8,9] or serine proteases.[10] Recently, thermophilic microorganism,[11] mesophilic bacteria,[12] fungi,[13] and thermophilic actinomycetes[14] isolated from various environments have been used to degrade PES successfully. Biodegradation rate is undoubtedly one of the most important properties of biodegradable polymers. Chemical structure, copolymer composition, crystalline structure, and morphology[5,7] influence the biodegradation rate. Lately, the degree of crystallinity[15] has been singled out as the factor that affects mostly biodegradation of polymers, because biodegradation firstly takes place in the amorphous region, such that the erosion proceeds at a higher rate in the

Additional Supporting Information may be found in the online version of this article

Correspondence to: M. Chen (mingchen@mail.nsysu.edu.tw).

Contract grant sponsor: National Science Council of Taiwan (ROC); contract grant number: NSC 96-2221-E-110-045.

amorphous region than in the crystalline region.[16,17] Hence, research on the relationship among structure, crystallization kinetics and morphology must precede research on degradation behavior, and the results thus obtained will help elucidate the degradation mechanism, supporting the design and development of various practical degradable polymers.

To promote the physical properties or extend the range of application of PES and PBS, there are numerous approaches have been employed, such as physical blending, copolymerization, and formation of composite with organoclay. PES was found to be miscible with poly(beta-hydroxybutyrate),[18] poly (ethylene oxide),[19–22] or poly(vinyl phenol),[23] and to be partially miscible with cellulose acetate,[24] poly (vinyl chloride),[25] or PBS.[26] However, PES blends with poly(3-hydroxybutyrate-*co*-hydroxyvalerate)[27] or poly(L-lactide)[28] were immiscible. Copolymers are well known to have higher degradation rates than homopolymers, which is basically attributed to the limited crystallinity.[29–31] In previous studies, it was found that the incorporation of trimethylene succinate units into PES significantly inhibited the crystallization behavior of PES and decreased its melting temperature.[32] To increase the biodegradation rate without sacrificing the melting temperature of succinates, PES copolymers with minor amounts of butylene succinate (BS) were synthesized in this work.[33–35] Blends of PES and PBS were prepared in chloroform with the weight ratios of PES/PBS: 98/02, 95/05, and 90/10 for the comparison with the copolymers. Over a wide range of isothermal crystallization temperature (T_c), the differential scanning calorimetry (DSC) data were analyzed using the Avrami equation.[36,37] Additionally, the origin of multiple melting behaviors of isothermal crystallized specimens was elucidated using wide-angle X-ray diffraction (WAXD) patterns and DSC curves. The thermal properties and the degree of crystallinity of both blends and copolymers were compared.

EXPERIMENTAL

Materials and specimen preparation

Ethylene glycol (EG) (Showa, 99.5%), 1,4-butanediol (BD) (Acros, 99%) and succinic acid (SA) (Acros, 99%) were used without purification. Titanium tetraisopropoxide (TTP) (Acros, 98+%) was used as received. Other solvents used in the analysis were also used without purification. PES, PBS, and PES-rich copolyesters were synthesized via a two-step esterification reaction in the melt. A detailed report of synthesis and characterization has been simply referred our most recent work.[33] The synthesized polyester was dissolved in chloroform and precipitated into 10 times the amount of vigorously stirred ice-cooled methanol. The precipitate was filtered, washed with methanol, and dried under reduced pressure at room temperature. The first column of Table I presents the sample codes of copolyesters (PEBSA) and blends (PES/PBS), with the numerical values representing the feed ratios of the diols or the weight ratios of PES and PBS.

TABLE I
Intrinsic Viscosity and Thermal Properties[33]

Sample code	[η] (dL/g)	T_g (°C)	T_{cc} (°C)	T_m' (°C)	T_m'' (°C)
PES[a]	1.08	−10.8	47.7	100.9	–
PBS[a]	1.27	−41.1	−15.5	–	113.1
PEBSA 95/05[a]	1.25	−11.7	53.3	94.5	–
PEBSA 90/10[a]	1.14	−14.2	56.3	89.8	–
PEBSA 50/50	1.18	−29.1[a]	–	37.8[b]	–
PES/PBS 98/02[a]		–	44.3	101.0	112.6
PES/PBS 95/05[a]		–	44.0	100.8	112.6
PES/PBS 90/10[a]		–	45.5	101.3	112.6
PES[c]	1.08	−10.4	28.0	105.1	–
PES/PBS 98/02[c]		−10.2	21.4	105.2	116.3
PES/PBS 95/05[c]		−10.1	21.6	105.3	116.4
PES/PBS 90/10[c]		−10.5	21.0	105.1	116.1

[a] at a heating rate of 10°C/min for amorphous specimen.
[b] at a heating rate of 10°C/min for room temperature annealed specimen.
[c] at a heating rate of 1°C/min for amorphous specimen using TMDSC. T_{cc}: cold crystallization peak temperature.

Purified polyester samples were dissolved in 60/40 w/w phenol/1,1,2,2-tetrachloroethane solution. The solution viscosities of the polyesters at 30°C were measured using an Ubbelohde viscometer. Their intrinsic viscosity, [η], values ranged from 1.08 to 1.27 dL/g, as listed in the second column of Table I.[33] PES had a [η] of 1.08 dL/g and a number average molecular weight of 1.05×10^5 g/mol relative to poly(methyl methacrylate).[32,38] In this study, PES, PBS, and PEBSA were synthesized using an effective catalyst, TTP, without the addition of any heat stabilizer. The molecular weights of these polyesters were high enough to allow them to be made into films for the subsequent studies. PES/PBS blends with different weight ratios were prepared by dissolving PES and PBS in chloroform (1 wt %), then chloroform was evaporated in hood after casting on petri dish. Dried blend or copolymer was sandwiched between two polyimide films with spacers, and was heated from room temperature to 20–30°C above its melting temperature (T_m). The sheet was formed by compression molding for 5 min at 5 kg/cm^2 pressure. During the molding process, the mold was pressed and released several times to ensure that the sheet was void-free. The sheet was then allowed to cool slowly to room temperature. The compressed sheet had a thickness of ~0.2 mm for use in DSC studies or about 0.5 mm for obtaining

WAXD patterns. All sheets were dried at room temperature in a vacuum oven overnight before they were used.

NMR and WAXD measurements

NMR spectra of *d*-chloroform solutions were recorded with tetramethylsilane as the reference standard using a Varian UNITY INOVA-500 NMR at 295.5 K. ^{1}H-NMR spectra were analyzed to determine the compositions of the copolyesters and PES/PBS 90/10 blend. ^{13}C-NMR was utilized for the determination of both the composition and the ester sequence distribution in these copolyesters.

Specimens with a thickness of about 0.5 mm, following complete isothermal crystallization at T_c, were prepared using a heating stage (Linkam THMS-600). X-ray diffractograms were obtained on a Siemens D5000 diffractometer with Ni-filtered Cu K_α radiation ($\lambda = 0.1542$ nm, 40 kV, 30 mA) at a scanning rate of 1°/min. Measurements were made at room temperature.

Measuring thermal properties and thermal stability

The thermal properties of the polyesters and blends were analyzed using a Perkin-Elmer Pyris 1 DSC, equipped with a refrigerating system (Pyris Intracooler 2P). Temperature was calibrated with deionized water and indium, and the heat flow was calibrated using indium. A specimen with a weight 4 ± 0.5 mg was used. It was initially heated at a rate of 20°C/min from 30 to 170°C for PES-rich polymers or to 180°C for the blends, at which temperature it was maintained in a molten state for 5 min to remove the thermal history. Subsequently, the specimen was quenched with liquid nitrogen and then heated at a rate of 10°C/min to above its T_m. The glass transition temperature (T_g), T_m and cold crystallization temperature (T_{cc}) were detected during the heating process.

For the blends, the T_g values of amorphous specimens were obtained from the reversible curves of temperature modulated DSC (TMDSC, TA Instruments Q100), equipped with a refrigerating system. The cell constant calibration was performed using an indium standard, and the temperature calibration was conducted using deionized water and indium. A standard sapphire sample was used to measure the calibration constant of heat capacity for the modulation study. A heating rate of 1°C/min with a period of 60 s and a modulation amplitude of 0.159°C were selected as a heating-only condition based on the specifications that are presented in the instrument manual.

Thermal stability experiments were conducted using a TA Instruments 2050 thermogravimetric analyzer (TGA). Nitrogen gas was used as the purge gas at a flow rate of 50 ml/min. A specimen of lighter than 10 mg was heated at a rate of 10°C/min from room temperature to 800°C. Weight loss curves and their derivatives were obtained to compare the relative thermal stabilities of the synthesized polyesters and PES/PBS blends.

Differential scanning calorimetry measurements

A Perkin-Elmer Pyris 1 DSC was used and calibrated as described above. About 3–5 mg of the blend was used. In the isothermal crystallization study, the samples were initially heated from 30 to 180°C at 20°C/min at which temperature they were maintained in a molten state for 5 min. They were then rapidly cooled at a nominal rate of 250°C/min to a preset temperature (T_c) between 30 and 88°C, and crystallized for a period that was three times the peak ending time to ensure complete crystallization. The enthalpy of crystallization exotherm was measured as a function of time, and the crystallization kinetics was analyzed by Avrami method.[36,37] Following isothermal crystallization, the specimens were scanned directly from T_c up to 140°C at 10°C/min to examine their melting behavior.

RESULTS AND DISCUSSION

NMR analysis

A detailed determination of the compositions and the ester sequence distribution of PEBSA copolymers were reported in our most recent work.[33] In the ^{13}C-NMR spectrum of PEBSA 50/50, the carbonyl carbons were split into four peaks, which areas were utilized for the determination of the triads possibility, composition and the ester sequence distribution in this copolyester. Based on the analysis of carbonyl carbons, PEBSA 90/10 copolyester was characterized as having 89.9 mol % ethylene succinate (ES) units and 10.1 mol % BS units in a random sequence.[34] Only enlarged ^{13}C-NMR spectrum of the carbonyl carbons of PEBSA 90/10 copolymer is replotted in Figure 1 for the comparison with PES/PBS 90/10 blend. The assigned "a" peak at 171.9–172.0 ppm refers to the carbonyl carbons of PES homopolymer with ES units on both sides of succinate unit. There are only two peaks for the carbonyl carbons of PES/PBS 90/10 blend. Another peak "d" at 172.2–172.3 ppm is assigned to the carbonyl carbons of PBS homopolymer with BS units on both sides of succinate unit. The composition of this blend is determined from the relative areas under these two peaks. The calculated result indicates that PES/PBS 90/10 blend has 88.8 mol % PES and 11.2 mol % PBS. The analyses of ^{1}H-NMR spectrum of PES/PBS

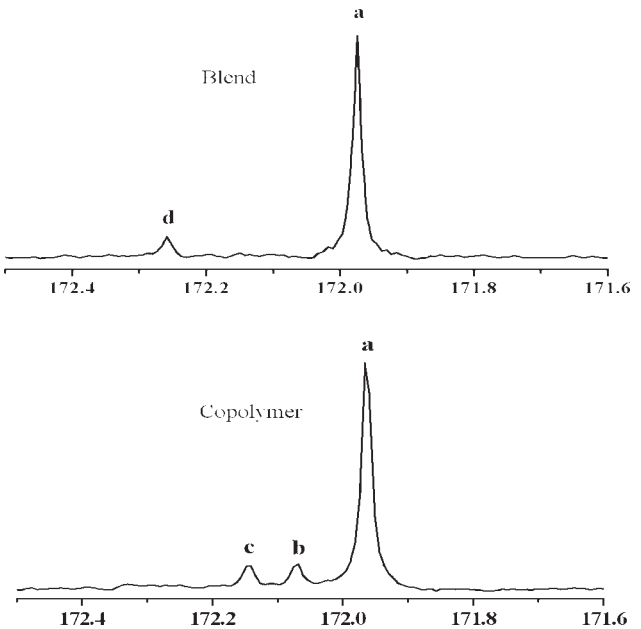

Figure 1 ^{13}C-NMR spectra of the carbonyl carbons of PES/PBS 90/10 blend and PEBSA 90/10 copolymer.

90/10 blend gives 89.0 mol % PES and 11.0 mol % PBS. Both results are in good agreement with those expected from the weight ratio of this blend.

Thermal properties

Figure 2 plots DSC heating curves of amorphous polyesters[33] and amorphous blends. PES has the highest T_g at −10.8°C. The T_g value slowly declines from −10.8 to −41.1°C as the moiety of the BS units increases from 0 to 100%, as presented in the third column of Table I. Such T_g depression is attributed to the increase in the chain flexibility by the incorporation of BS units. For the blends, the peak at T_{cc} of

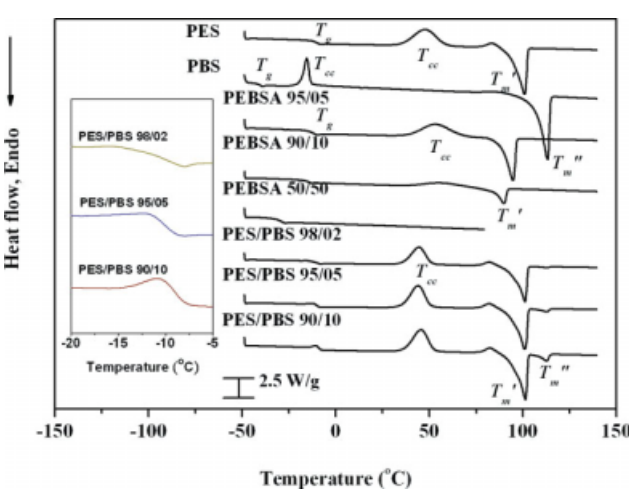

Figure 2 DSC thermograms of amorphous polyesters and blends at a heating rate of 10°C/min. [Color figure can be viewed in the online issue, which is available at www.interscience.wiley.com.]

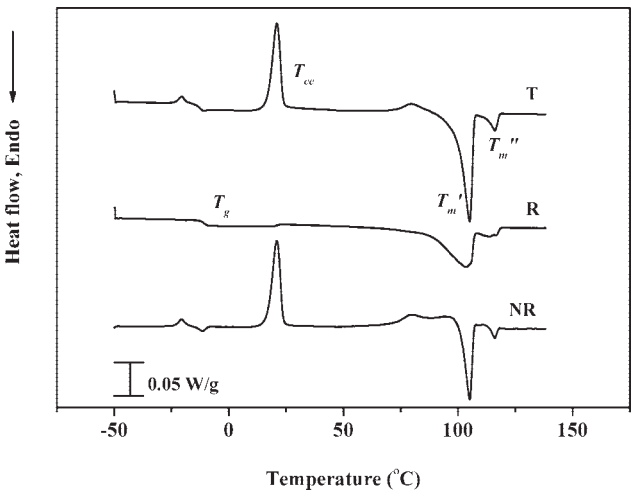

Figure 3 TMDSC thermograms of amorphous PES/PBS 90/10 blend at a heating rate of 10°C/min.

PBS overlaps with the glass transition of PES, as shown in the inset thermograms of Figure 2. Hence, TMDSC was used to separate them. Figure 3 shows the TMDSC curves at a heating rate of 1°C/min for amorphous PES/PBS 90/10 blend. The total heat flow (abbreviated as T) could be qualitatively separated into the heat capacity related component (reversible, as R) and the kinetic component (non-reversible, as NR). A distinct glass-rubber transition is observed in the reversible curve. For PES neat polymer, this transition temperature, −10.4°C, is very close to −10.8°C, as determined at a heating rate of 10°C/min using conventional DSC. Hence, the transition temperature which is obtained from the reversible curve is designated as the T_g of PES/PBS blend. The T_g values of the blends are also tabulated in the third column of Table I for comparison. These blends keep the intrinsic T_g of PES neat polymer with a value ranging from −10.5 to −10.1°C. The preliminary results of the phase contrast optical microscopy of PES/PBS 95/5 blend in the melt state showed the behavior of phase separation (Supporting Information Figures S1 and S2). Therefore, the slight variation of the T_g values with the blend composition indicates that PES and PBS could be

TABLE II
Thermal Stability and Equilibrium Melting Temperature[33–35]

Sample code	T_{start} (°C)	$T_{loss2\%}$ (°C)	T_{max} (°C)	T_m^0 (°C)
PES	247.1	291.9	379.5	112.7
PBS	246.1	298.5	400.3	127.4
PEBSA 95/05	248.1	283.9	387.4	111.1
PEBSA 90/10	242.1	277.9	398.2	107.0
PEBSA 50/50	241.1	285.4	404.5	–
PES/PBS 98/02	247.1	286.7	382.9	113.2
PES/PBS 95/05	243.3	286.4	395.6	113.0
PES/PBS 90/10	245.8	288.2	388.4	113.2
Average	245.1 ± 2.6	287.4 ± 6.0	392.1 ± 8.9	

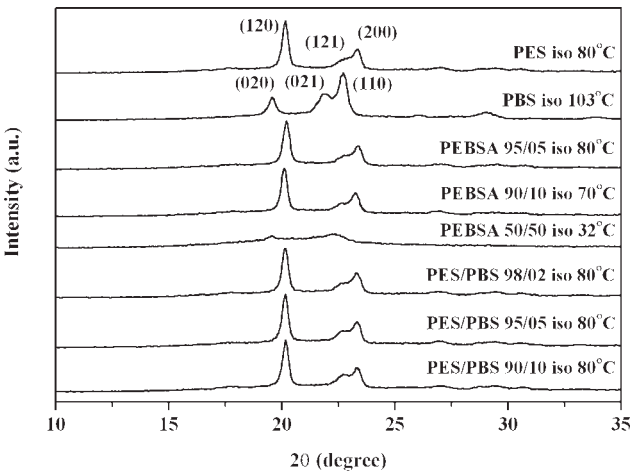

Figure 4 WAXD patterns from polyesters and blends crystallized isothermally at the temperatures indicated.

immiscible in the amorphous phase. This phenomenon will be further discussed in the next manuscript.

A sharp cold crystallization peak occurs at −15.5°C for PBS homopolymer, suggesting that the cold crystallization rate of PBS markedly exceeds that of PES homopolymer. As mentioned above, the cold crystallization peak of PBS in the PES/PBS blend overlaps with the glass transition of PES (Fig. 2). For all the DSC curves of these PES/PBS blends, a narrower cold crystallization peak is also observed around 45°C, which is 3°C earlier than the cold crystallization peak of PES homopolymer. It seems that PES was not effectively nucleated by the few PBS crystals. The T_m' value of these three blends keeps around 101°C, which is the melting temperature of PES homopolymer. A small melting peak is detected at 112.6°C (T_m''), which is the melting temperature of PBS homopolymer. Table I also tabulates the values of T_{cc}, T_m' and T_m'' obtained from the total heat flow of TMDSC curve at a heating rate of 1°C/min. The T_{cc} value of PES is about 23°C less (or the cold crystallization occurs earlier), and the T_m' and T_m'' values are ~4°C higher.

A cold crystallization peak (T_{cc} at 47.7°C) and a small recrystallization peak just before the melting peak (T_{m1} at 100.9°C) are detected for PES homopolymer, as presented in Figure 2. For PEBSA 95/05 and 90/10 copolymers,[33] T_{cc} moves from 53.3 to 56.3°C (fourth column in Table I) and the corresponding peak becomes lower and broader. No cold crystallization is revealed by the curve of PEBSA 50/50. Clearly, the incorporation of a few BS units into PES reduces the cold crystallization rate of amorphous specimens. Accordingly, the intensity of the melting peak declines, and the corresponding T_m' falls from 100.9, through 94.5 to 89.8°C, as indicated in the fifth column of Table I. Increasing the fraction of BS units to 50 mol % (PEBSA 50/50) decreased T_m' drastically to 37.8°C that was obtained after the specimen was kept at room temperature for more than 3 days.

Thermal stability

For brevity, TGA curves of the weight loss and the derivative of weight loss versus temperature are not shown here. Table II presents three temperature parameters for all of the polyesters[33] and blends used in this study, along with their average values, where T_{start} is the temperature of first detectable deviation from the derivative curve of weight loss, $T_{loss2\%}$ represents the temperature at a weight loss of 2% from the weight loss curve, and T_{max} denotes the temperature with the greatest slope from the weight loss curve. The average values of T_{start}, $T_{loss2\%}$, and T_{max} are 245.1 ± 2.6°C, 287.4 ± 6.0°C, and 392.1 ± 8.9°C, respectively. The values of $T_{loss2\%}$ are well above 220°C, the temperature of the last step of synthesis.[33] It can be assumed that no appreciable thermal degradation took place during the step of polycondensation, so there was no need to use a heat stabilizer during the synthesis of these polyesters. Additionally, these polyesters and blends exhibit no significant variation or no trend in these three temperature parameters because this experiment depends on the size, shape, and the degree of crystallinity of the specimens. Similar results have been reported for a series of PEBSA copolymers.[30]

Wide-angle x-ray diffraction

Figure 4 shows the diffraction diagrams of PES, PBS, PEBSA copolyesters[33] and PES dominated blends that were isothermally crystallized at 5–20°C below

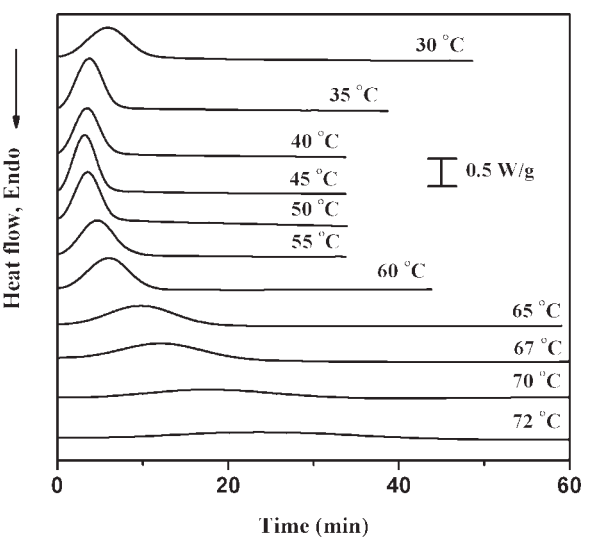

Figure 5 Crystallization isotherms of PES/PBS 90/10 blend at the indicated temperatures (T_c).

TABLE III
Summary of the Condition and the Kinetic Analysis of Crystallization for Isothermally Crystallized PES/PBS 90/10 Blend

T_c (°C)	t_c (min)	ΔH_{exo} (J/g)	ΔH_{endo} (J/g)	$X_{c,endo}$ (%)	$t_{1/2}$ (min)	n_1	k_1 (min^{-n})
30	50	−40.8	54.8	32.6	5.88	2.88	4.21×10^{-3}
35	40	−42.5	54.9	32.7	3.69	2.81	1.78×10^{-2}
40	35	−41.7	55.1	32.8	3.50	2.76	2.36×10^{-2}
45	35	−43.3	56.8	33.8	3.17	2.78	2.82×10^{-2}
50	35	−43.5	56.8	33.8	3.55	2.84	1.89×10^{-2}
55	35	−44.6	57.3	34.1	4.70	2.79	9.15×10^{-3}
60	45	−44.7	57.7	34.3	5.94	2.98	3.53×10^{-3}
65	60	−45.9	58.6	34.9	9.76	2.97	8.05×10^{-4}
67	100	−46.6	58.6	34.9	11.93	3.03	3.87×10^{-4}
70	150	(−40.8)	59.3	35.3	16.14	2.84	2.67×10^{-4}
72	250	(−34.3)	61.2	36.4	22.19	2.79	1.23×10^{-4}
75	300	–	61.3	36.5	–	–	–
80	700	–	62.5	37.2	–	–	–
85	1000	–	64.9	38.7	–	–	–
88	1200	–	(49.2)	(−29.3)	–	–	–

their respective T_m values. The unit cell of the crystalline PES α form is orthorhombic,[7,39] and the diffraction peaks from the (120) and (200) planes are observed at $2\theta \approx 20.2^\circ$ and 23.4°, respectively. PEBSA 95/05 and 90/10 copolyesters have diffraction peaks of the PES α form, but their intensity from the (120), (200) and (121) planes decreases as the moiety of the BS units increases, indicating less crystalline order in these copolymers. The unit cell of the crystalline PBS α form is monoclinic,[40,41] and the diffraction peaks from the (020) and (110) planes are observed at $2\theta \approx 19.6^\circ$ and 22.7°, respectively. The diffraction diagram of PEBSA 50/50 has the characteristic peaks of the PBS α form, but with very low intensity. All PES dominated blends have more pronounced diffraction peak from the (121) plane of PES crystals [may be part from the (110) plane of PBS crystals] than that of copolymer, indicating improvement of crystalline order in the blends.

Isothermal crystallization kinetics

Detailed studies of isothermal crystallization kinetics of PEBSA copolymers were reported in our most recent works.[34,35] For brevity, only the kinetic analysis of PES/PBS 90/10 blend is presented here. Figure 5 displays DSC exothermic traces for the specimens that were isothermally crystallized at temperatures from 30 to 72°C. DSC traces are not presented for T_c above 72°C, because the exothermic heat flow becomes too slow and small to be accurately defined for the ending time of the crystallization process. The second column in Table III shows isothermal crystallization times (t_c) at temperatures from 30 to 88°C. The required t_c decreased from 55 min at 30°C to 35 min at temperatures between 40 and 55°C, and then increased gradually to 300 min at 75°C, reaching 1200 min at 88°C. The exothermic heat flow was integrated to yield the heat of crystallization (ΔH_{exo}, third column). The relative degree of crystallinity at time t [$X_c(t)$] was calculated for each T_c. The half-time of crystallization ($t_{1/2}$ — defined as the time required for half of the final crystallinity to develop) was evaluated. The value of $t_{1/2}$ falls from 5.88 min at 30°C to 3.17 min at 45°C, and then increases gradually to 22.19 min at 72°C, as listed in column 6 of Table III. Figure 6 plots the overall crystallization rate ($t_{1/2}{}^{-1)}$ versus temperature (T_c) as solid right triangles.

It is well known that the Avrami equation[36,37] can be applied to describe the initial or the primary stage of isothermal crystallization of polymers, as followed:

$$1 - X_c(t) = \exp(-k_1 t^{n_1}) \quad (1)$$

$$\log[-\ln(1 - X_c(t))] = \log\ k_1 + n_1\ log\ t \quad (2)$$

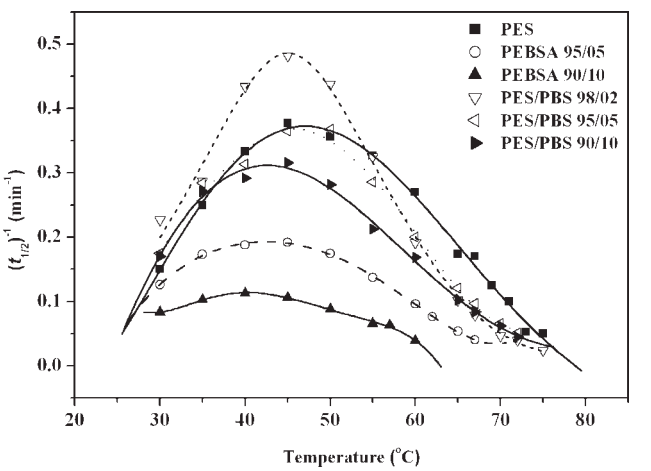

Figure 6 Temperature dependencies (T_c) of the overall crystallization rate ($t_{1/2}{}^{-1}$).

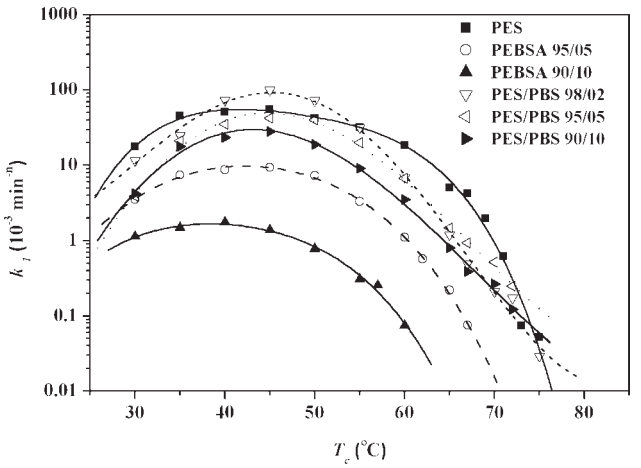

Figure 7 Temperature dependencies (T_c) of the rate constant (k_1).

where k_1 denotes the crystallization rate constant and n_1 is the Avrami exponent describing the crystal geometry and nucleation mechanism. According to eq. (2), the plot of $\log[-\ln(1 - X_c(t))]$ versus $\log t$ yields the slope n_1 and the intercept $\log k_1$. The last two columns in Table III tabulate the data of n_1 and k_1 at different T_c values for PES/PBS 90/10 blend. As T_c increases, n_1 falls initially from 2.88 at 30°C to 2.76 at 40°C, and then increases to 3.03, as presented in column 7 in Table III. The k_1 value increases first from 4.21×10^{-3} min^{-n} at 30°C to 2.82×10^{-2} min^{-n} at 45°C, and then declines to 1.23×10^{-4} min^{-n}; the results are listed in the last column of Table III and also plotted as solid right triangles in Fig. 7.

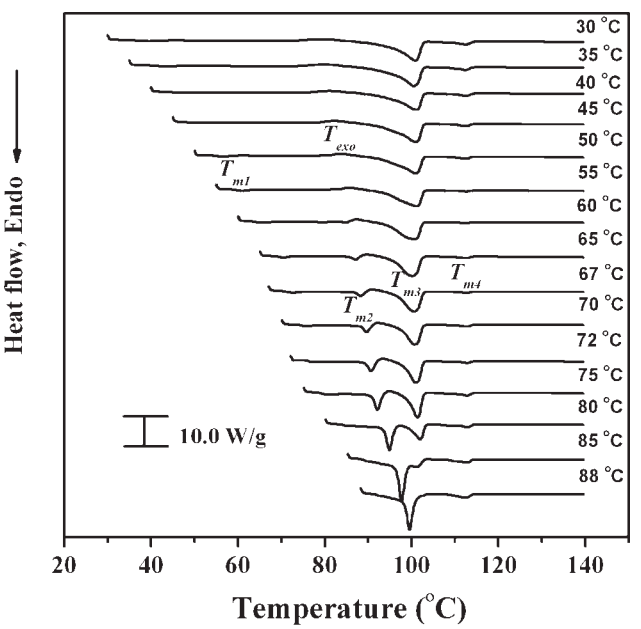

Figure 8 DSC thermograms (at a heating rate of 10 °C/min) for PES/PBS 90/10 blend isothermally melt-crystallized at the indicated temperatures.

For the isothermal crystallization experiments of PES/PBS 98/02 and 95/05 blends, a similar t_c value as that of PES/PBS 90/10 blend was selected for each T_c ranging from 30 to 88°C. The kinetic analysis based on the Avrami equation gives n_1 values between 2.57 and 2.99. The n_1 values of these blends are larger than those of the corresponding copolymers. These n_1 values are less than 4.0, because, first, the thickness of the samples for the DSC studies was about 0.2 mm. At higher T_c values, the nucleation density was low, and the diameter of the spherulite was around 0.1 mm.[34,35,42] Hence, the growth of the spherulites was restricted to two dimensions during the latter stage of isothermal crystallization. Next, the spherulitic growth rate of these PES dominated blends is low.[38] The primary and secondary crystallizations are suggested to proceed simultaneously before the impingement of the crystals.[35] Third, the homogeneous nucleation rate increases at lower T_c, representing an athermal nucleation process that is followed by three-dimensional crystal growth in the initial stage of isothermal crystallization. Finally, the cooling rate of the refrigerating system is not high enough to prevent the crystallization of PBS (and a little of PES) before it is cooled to a low T_c. Similar results were observed in the earlier studies for PES-rich copolyesters.[34,35,42] Figures 6 and 7 display the temperature dependencies of the overall crystallization rate ($t_{1/2}{}^{-1)}$ and the rate constant (k_1), respectively, for PES,[42] PEBSA copolymers[34,35] and PES/PBS blends. Both plots present a maximum value at ~45°C for all of these specimens. It is reasonable that the overall crystallization rate ($t_{1/2}{}^{-1}$) is maximal at a temperature between the temperatures of the maximum nucleation rate and the maximum growth rate in PES-rich copolymers[34,35,42] and PES dominated blends. Figures 6 and 7 also indicate that PEBSA 90/10 copolymer has the lowest overall crystallization rate and the lowest rate constant.

Elucidating the melting behavior and the degree of crystallinity

The melting behavior of PEBSA copolymers[34,35] following isothermal crystallization was investigated

TABLE IV
Degree of Crystallinity Obtained from DSC Endothermic Heating Curves[34,35]

T_c (°C)	PES	PEBSA 95/05	PEBSA 90/10	PES/PBS 98/02	PES/PBS 95/05	PES/PBS 90/10
30	31.4	32.3	29.0	32.4	34.1	32.6
40	31.8	29.7	30.0	33.2	34.9	32.8
50	33.8	30.7	30.2	33.8	35.1	33.8
60	34.0	31.3	30.8	34.0	35.3	34.3
70	35.2[a]	32.9	31.6	35.4	35.5	35.3
80	37.5	33.2	--	36.7	37.4	37.2

[a] Isothermal crystallization at 71°C.

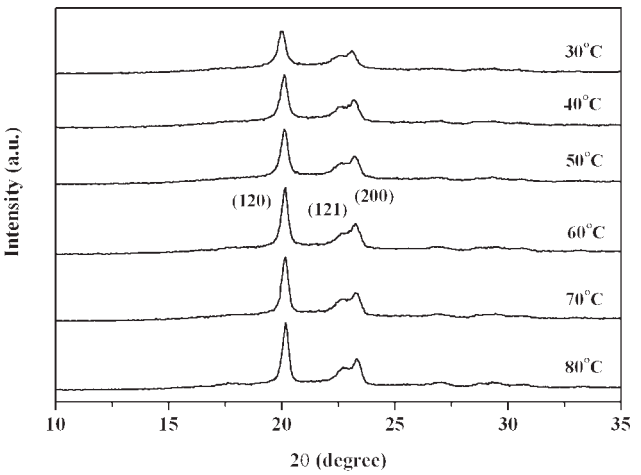

Figure 9 X-ray diffraction patterns of PES/PBS 90/10 blend isothermally crystallized at various temperatures.

using DSC by varying the T_c, the heating rate and the crystallization time. DSC curves showed triple melting peaks. The peak temperatures of the melting peaks are denoted T_{m1}, T_{m2} and T_{m3} in order of increasing temperature (as in Fig. 8). The lower temperature part of the peak at T_{m3} is related to the melting of the recrystallized crystals.[42] As T_c increases, the contribution of the melting–recrystallization–remelting process to the peak at T_{m3} gradually falls and finally disappears.[34,42] The peak at T_{m1} is associated with the secondary crystals.[35] Figure 8 displays the results of DSC heating scans at a heating rate of 10°C/min for PES/PBS 90/10 blend. The heating curves show one additional melting peak (T_{m4} for PBS) along with triple endothermic peaks. The peak at T_{m2} is attributed to the fusion of the crystals that are grown during the primary crystallization.[34,35,42] A Hoffman–Weeks[43] linear plot gives an equilibrium melting temperature (T_m^0) of 113.2°C, as listed in the last column of Table II. The T_m^0 values of PES,[38] PBS, PEBSA copolymers[34,35] and PES/PBS blends are also tabulated in the same column. These three blends have almost the same T_m^0 value, but copolymer has a lower T_m^0 value as the moiety of the BS units increases.

DSC traces in Figure 8 are integrated to yield the net enthalpies of melting (ΔH_{endo}) which are tabulated in the fourth column of Table III. Its value increases from 54.8 to 64.9 J/g as T_c increases from 30 to 85°C. The degree of crystallinity ($X_{c,exo}$) is determined by dividing the net enthalpy of melting (ΔH_{endo}) by 163 J/g,[33] the theoretical value for fully (100%) crystalline PES evaluated from the Flory equation.[44] $X_{c,exo}$ increases from 32.6 to 38.7%, as shown in the fifth column of Table III. The degrees of crystallinity evaluated from the net enthalpies of melting are listed in Table IV at various T_c values for the comparison among PES,[42] PEBSA copolymers[34,35] and PES/PBS blends. It can be found clearly that PEBSA 90/10 copolymer displays the lowest degree of crystallinity.

Figure 9 shows the diffraction diagrams of PES/PBS 90/10 blend following crystallization at various isothermal temperatures (T_c). All the samples show the same PES diffraction peaks over the entire range of temperatures, revealing only one crystalline form (α) in the samples that were crystallized isothermally between 30 and 80°C. As the T_c increases, the diffraction peak from the (120) plane becomes sharper and the width at half-maximum peak decreases gradually. The mean crystal sizes L_{hkl}, perpendicular to the (hkl) plane, can be estimated with the familiar Scherrer equation, as follows:[45]

$$L_{hkl} = \frac{K\lambda}{\beta_0 \cos\theta} \tag{3}$$

where β_0 is the breath at half-maximum peak corrected for instrumental broadening and K denotes the Scherrer factor. L_{hkl} was strongly dependent on the peak broadening (β_0). However, the numerical values obtained from eq. (3) are not accurate because of the prevalence of lattice distortions. Figure 9 reveals that the sizes or the lamellar thickness of the crystals increase with increasing T_c. Additionally, the diffraction peak from the (200) plane also becomes sharper and the diffraction peak of the (121) plane turns out to be more pronounced, indicating improvement of crystalline order. The crystallinity of this blend increased from 29.4 to 34.2% (see the last column in Table V), as determined from the relative areas under the crystalline peaks and the amorphous background using the Jade software. The crystallinity of PEBSA copolymers[34,35] and PES/PBS blends at various T_c values are also tabulated in Table V for the comparison. It also indicates that PEBSA 90/10 copolymer has the lowest crystallinity.

CONCLUSIONS

The results of intrinsic viscosity measurements and thermal stability experiments indicate high-

TABLE V
Crystallinity Evaluated from WAXD Patterns Using the Jade Software

T_c(°C)	PEBSA 95/05	PEBSA 90/10	PES/PBS 98/02	PES/PBS 95/05	PES/PBS 90/10
30	27.5	26.5	29.0	31.2	29.4
40	27.7	26.8	30.2	31.9	30.3
50	28.2	27.7	31.2	32.4	31.2
60	28.6	28.1	31.9	32.7	32.1
70	29.0	29.1	32.6	33.3	33.0
80	30.7	–	34.1	34.6	34.2

molecular weight PES, PBS, and PEBSA copolymers can be synthesized using an effective catalyst, TTP, without the addition of any heat stabilizer in this study. NMR spectra show that the compositions of the copolymers or the blends are in good agreement with those expected from the feed ratio of diols or the weight ratio of homopolymers. There is a single T_g detected in the blends, and a small variation of the T_g values with the blend composition. The miscibility of these PES/PBS blends will be discussed in the next manuscript. The kinetic analysis of the isothermal crystallization data of these polyesters and blends presents a maximum temperature at around 45°C from both the plots of the temperature dependencies of the overall crystallization rate and the rate constant. PEBSA 90/10 copolyester has the lowest rate and the lowest rate constant. After isothermal crystallization of these samples, the degree of crystallinity evaluated from DSC melting traces or WAXD patterns also shows that PEBSA 90/10 copolyester has the lowest value. However, PES/PBS 98/2, 95/5 and 90/10 blends keep the melting temperature and the crystallinity of PES homopolymer.

References

1. Chandra, R.; Rustgi, R. Prog Polym Sci 1998, 23, 1273.
2. Tokiwa, Y.; Pranamuda, H. In Biopolymers; Doi, Y., Steinbüchel, A., Eds.; Wiley-VCH: Weinheim, 2001; Vol. 3b, p 85.
3. Fujimaki, T. Polym Degrad Stab 1998, 59, 209.
4. Kasuya, K.; Ohura, T.; Masuda, K.; Doi, Y. Int J Biol Macromol 1999, 24, 329.
5. Iwata, T.; Doi, Y. Macromol Chem Phys 1999, 200, 2429.
6. Gan, Z. H.; Abe, H.; Doi, Y. Biomacromolecules 2000, 1, 713.
7. Iwata, T.; Doi, Y.; Isono, K.; Yoshida, Y. Macromolecules 2001, 34, 7343.
8. Tsutsumi, C.; Hayase, N.; Nakagawa, K.; Tanaka, S.; Miyahara, Y. Macromol Symp 2003, 197, 431.
9. Bikiaris, D. N.; Papageorgiou, G. Z.; Achilias, D. S. Polym Degrad Stab 2006, 91, 31.
10. Lim, H. A.; Raku, T.; Tokiwa, Y. Biotechnol Lett 2005, 27, 459.
11. Tansengco, M. L.; Tokiwa, Y. World J Microbiol Biotechnol 1998, 14, 133.
12. Tezuka, Y.; Ishii, N.; Kasuya, K. I.; Mitomo, H. Polym Degrad Stab 2004, 84, 115.
13. Ishii, N.; Inoue, Y.; Shimada, K. I.; Tezuka, Y.; Mitomo, H.; Kasuya, K. I. Polym Degrad Stab 2007, 92, 44.
14. Hoang, K. C.; Tseng, M.; Shu, W. J. Biodegradation 2007, 18, 333.
15. Mochizuki, M.; Hirami, M. Polym Adv Technol 1997, 8, 203.
16. Kumagai, Y.; Kanesawa, Y.; Doi, Y. Makromol Chem Macromol Chem Phys 1992, 193, 53.
17. Abe, H.; Doi, Y.; Aoki, H.; Akehata, T. Macromolecules 1998, 31, 1791.
18. Al-Salah, H. A. Polym Bull 1998, 41, 593.
19. Chen, H. L.; Wang, S. F. Polymer 2000, 41, 5157.
20. Qiu, Z. B.; Ikehara, T.; Nishi, T. Macromolecules 2002, 35, 8251.
21. He, S. A.; Liu, J. P. Polym J 2007, 39, 537.
22. Lu, J. M.; Qiu, Z. B.; Yang, W. T. Macromolecules 2008, 41, 141.
23. Qiu, Z. B.; Fujinami, S.; Komura, M.; Nakajima, K.; Ikehara, T.; Nishi, T. Polymer 2004, 45, 4515.
24. Buchanan, C. M.; Pearcy, B. G.; White, A. W.; Wood, M. D. J Environ Polym Degrad 1997, 5, 209.
25. Abdel-Naby, A. S.; El Hefnawy, M. Polym Test 2003, 22, 25.
26. Papageorgiou, G. Z.; Bikiaris, D. N. J Polym Sci Part B: Polym Phys 2006, 44, 584.
27. Miao, L. Q.; Qiu, Z. B.; Yang, W. T.; Ikehara, T. React Funct Polym 2008, 68, 446.
28. Lu, J. M.; Qiu, Z. B.; Yang, W. T. Polymer 2007, 48, 4196.
29. Mochizuki, M.; Mukai, K.; Yamada, K.; Ichise, N.; Murase, S.; Iwaya, Y. Macromolecules 1997, 30, 7403.
30. Cao, A.; Okamura, T.; Nakayama, K.; Inoue, Y.; Masuda, T. Polym Degrad Stab 2002, 78, 107.
31. Gan, Z.; Abe, H.; Doi, Y. Biomacromolecules 2001, 2, 313.
32. Tsai, C. J.; Chang, W. C.; Chen, C. H.; Lu, H. Y.; Chen, M. Eur Polym J 2008, 44, 2339.
33. Chen, C. H.; Lu, H. Y.; Chen, M.; Peng, J. S.; Tsai, C. J.; Yang, C. S. J Appl Polym Sci 2009, 111, 1433.
34. Lu, H. Y.; Lu, S. F.; Chen, M.; Yang, C. S.; Chen, C. H.; Tsai, C. J. J Polym Sci Part B: Polym Phys 2008, 46, 2431.
35. Lu, H. Y.; Lu, S. F.; Chen, M.; Chen, C. H.; Tsai, C. J. J Appl Polym Sci 2009, 113, 876.
36. Avrami, M. J Chem Phys 1939, 8, 212.
37. Avrami, M. J Chem Phys 1941, 9, 177.
38. Lu, H. Y.; Peng, J. S.; Chen, M.; Chang, W. C.; Chen, C. H.; Tsai, C. J. Eur Polym J 2007, 43, 2630.
39. Ueda, A. S.; Chatani, Y.; Tadokoro, H. Polym J 1971, 2, 387.
40. Ihn, K. J.; Yoo, E. S.; Im, S. S. Macromolecules 1995, 28, 2460.
41. Ichikawa, Y.; Kondo, H.; Igarashi, Y.; Noguchi, K.; Okuyama, K.; Washiyama, J. Polymer 2000, 41, 4719.
42. Chen, M.; Chang, W. C.; Lu, H. Y.; Chen, C. H.; Peng, J. S.; Tsai, C. J. Polymer 2007, 48, 5408.
43. Hoffman, J. D.; Weeks, J. J. J Res Natl Bur Stand 1962, 66A, 13.
44. Flory, P. J. Principles of Polymer Chemistry; Cornell University Press: Ithaca, NY, 1953; p 569.
45. Alexander, L. E. X-ray Diffraction Methods in Polymer Science; Krieger: Huntington, NY, 1969; p 423.